From Cellulose Solutions to Aerogels and Xerogels: Controlling Properties for Drug Delivery

Loris Gelas, Tatiana Budtova

From cellulose solutions to aerogels and xerogels: controlling properties for drug delivery

*Loris Gelas, Tatiana Budtova**

Mines Paris, PSL University, Center for Materials Forming (CEMEF), UMR CNRS 7635, CS 10207, 06904 Sophia Antipolis, France

Corresponding author: Tatiana Budtova

Tatiana.budtova@minesparis.psl.eu

ABSTRACT

Cheap and easy-to-recycle solvent, aqueous NaOH with no additives, was used to dissolve cellulose and make crosslinker-free materials of various porosity, testing them as drug delivery devices. Cellulose solutions were gelled, coagulated in a non-solvent (water, ethanol) and dried either using supercritical CO_2 (aerogels) or low-vacuum evaporation (named "xerogels"). Aerogels were of density around 0.1 g/cm³ and specific surface area (SSA) 200-400 m²/g. A significant influence of the first non-solvent and of drying mode on material properties was recorded: when the first non-solvent was ethanol and low-vacuum drying performed from ethanol, aerogel-like xerogels were obtained with density around 0.2 g/cm³ and SSA of 200-260 m²/g. Other conditions resulted in cellulose with much lower porosity and SSA. All materials were evaluated as drug delivery devices in simulated gastro-intestinal fluids; theophylline was used as a model drug. Materials of high porosity exhibited shrinking and rapid drug release whereas denser materials were swelling and showed slower release. Two release mechanisms were suggested: a diffusion-driven through aqueous media in the pores, and diffusion through swollen pore walls. The results demonstrate a large spectrum of options for tuning the properties of porous cellulose materials for drug release applications.

KEYWORDS: density, specific surface area, drying, evaporation, drug release, cellulose II

INTRODUCTION

The demand for efficient drug carriers never ceases to increase. An ideal carrier should be able to deliver the drug in the required quantity, to the right spot and for the appropriate duration. The delivery matrix should be biocompatible, easy to manufacture on a large scale and, if possible, cost effective. The most common way to administrate a drug into human body is by the oral route through the gastrointestinal track. This delivery mode has the advantages of being non-invasive, cost effective, and well known. Numerous strategies have been developed to tune the release kinetics of the drug, such as modification of the drug state, adjustment of the type, size, composition and properties of the delivery matrix (solubility, hydrophilic-lipophilic properties, porosity, pH- or temperature-responsiveness, etc) and tuning drug-matrix interactions[1–3].

The most prevalent drug delivery system involves a device in which the drug is uniformly dispersed. Traditional methods for producing such a loaded matrix include the compression or extrusion of excipients combined with active pharmaceutical ingredients[4]. The carrier material can exhibit responsiveness to the release medium, i.e. swelling, shrinking, erosion, or dissolution, thereby influencing drug release kinetics[5]. Among the various excipients utilized for pellet formulation, microcrystalline cellulose (MCC) is one of the most common. MCC, a widely available biopolymer, is renewable, non-toxic, and biodegradable. It comprises crystalline particles of few tens of microns, produced through the acid hydrolysis of cellulose fibers[6]. Upon oral administration, MCC-based tablet disperses, facilitating the rapid release of the drug from seconds to minutes, depending on the material's porosity and the presence of additives and/or binders[7].

Many pharmaceutical applications use porous materials as adjusting porosity and, also, polymer solubility, allows fine-tuning drug release kinetics. Porous materials can be “wet”, i.e. gels or hydrogels, or dry, obtained either by solvent sublimation from the gel, or by solvent evaporation, or by evacuation in supercritical conditions. Compared to gels and hydrogels, the advantage of dry

porous materials is that they are lightweight, do not require protection against bacteria and are stable in time as the dissolution or degradation of the matrix itself does not occur. Among dry porous materials, bio-aerogels make a special class of promising drug carriers as aerogels are of low-density, nanostructured, with pores' dimensions from few tens to few hundreds of nanometers; the majority of bio-aerogels do not involve any undesirable compounds either during formulation or processing[8].

Numerous research articles suggest using cellulose-based hydrogels and aerogels for drug delivery[9–13], but the majority focuses on nanocellulose-based systems (micro- or nanofibrillated, nanocrystals, bacterial cellulose). The reason of avoiding cellulose II hydrogels and aerogels is cellulose solvents which traces may be toxic or not allowed/not tested for biomedical applications. The exception is aqueous 7-9% NaOH solvent. Making cellulose fibers and films from cellulose/NaOH/water solutions on the large industrial scale is questionable because of sub-zero temperature of cellulose dissolution conditions, solution spontaneous gelation with time and temperature and low limit of cellulose solubility[14]. However, the use of this solvent for making high added-value porous cellulose for biomedical and pharmaceutical applications should be feasible. In addition, spontaneous gelation may be an advantage for shaping cellulose objects, and low cellulose concentration is required for making porous materials. Surprisingly, very few studies consider dry porous cellulose made by dissolution in NaOH/water as drug delivery device. Freeze-dried cellulose (density 0.05 – 0.12 g/cm^3) made from MCC dissolved in 8% NaOH/water, chemically crosslinked with epichlorohydrin or not, was used as a carrier of procaine hydrochloride[15]. The release of model molecules, methyl blue, rhodamine B and fluorescein, was monitored from cellulose aerogels (density 0.188 g/cm^3, specific surface area 100 – 180 m^2/g), but they were made by dissolving cellulose in 60% zinc chloride/water, coagulating in isopropanol, and drying with supercritical CO_2[13]. Interpenetrated pectin-cellulose aerogels (density 0.10 – 0.22

g/cm^3, specific surface area 300 to 500 m^2/g) were reported for the release of theophylline: cellulose was dissolved in 8 wt% NaOH/12 wt% urea/water, coagulated in water, impregnated with pectin solution, coagulated in ethanol and dried with supercritical CO_2[16]. Despite the discovery of cellulose aerogels about 20 years ago[17], with the first ones made by the dissolution in aqueous NaOH[18,19], very few studies report on their use as a delivery matrix[13, 20].

The goal of this work was to demonstrate that by fine-tuning processing pathways, cellulose materials with a large spectrum of porosity (from few to 95%) and surface area (from few to 400 m^2/g) can be made from the same starting cellulose-8%NaOH/water solution, with no additive and no crosslinker. To vary material properties, different coagulation pathways were applied (using only water and ethanol), and drying was performed either with supercritical CO_2 or by low-vacuum evaporation, the latter significantly simplifying the process of making cellulose aerogel-like materials. Material morphology and properties were correlated with the processing conditions, and materials obtained were tested as drug delivery matrix.

MATERIALS AND METHODS

Materials

Microcrystalline cellulose, particle average size 50 μm, was purchased from Thermo Fisher Scientific; the degree of polymerization was found to be 280 (see Figure S1 of the Supporting Information). Monobasic potassium phosphate (KH_2PO_4) (≥ 99%), sodium hydroxide pellets (NaOH), hydrochloric acid (HCl) (32 wt%), anhydrous theophylline (≥ 99%) and absolute ethanol (≥ 99%) were purchased from Sigma-Aldrich. All chemicals were used as received. Water was distilled.

Methods

Preparation of cellulose solutions and gels

The pathways of samples preparation is summarized in Figure 1. The first step consists of cellulose dissolution in aqueous 8 wt% NaOH/water at -6°C and 300 rpm during 1 h. Two cellulose concentrations were prepared, 3 and 5 wt%. 5 g of the obtained solution was then poured in a cylindrical mould and placed in oven at 50°C for 5 h; under these conditions cellulose solutions are gelling[21].

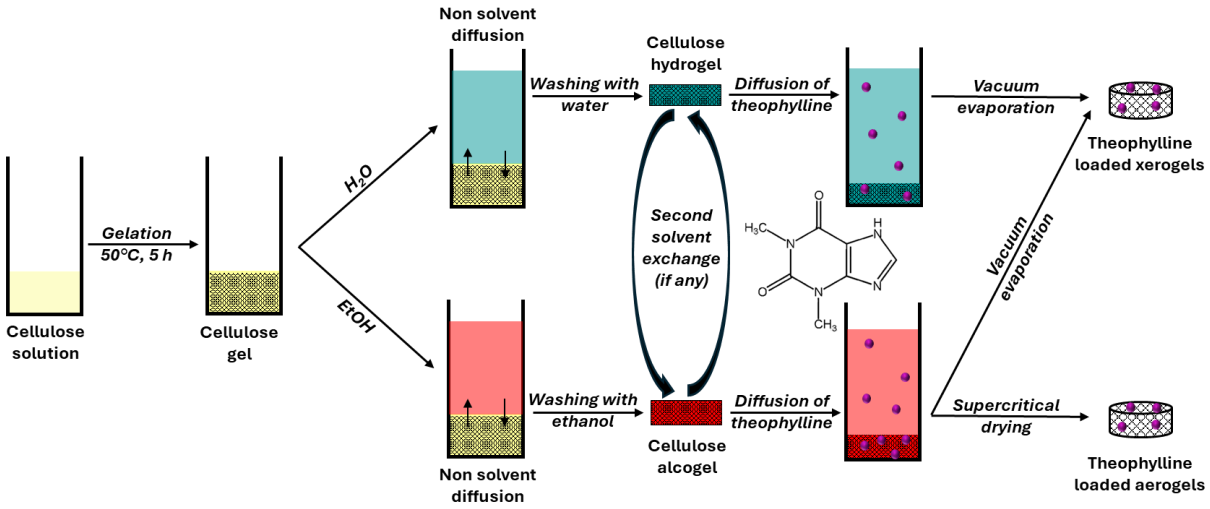

Figure 1. Schematic presentation of aerogels and xerogels preparation from 3 or 5 wt% cellulose/NaOH/water solutions loaded with theophylline.

Cellulose coagulation

The NaOH solution was washed out from cellulose gel by adding 40 mL of non-solvent, water or ethanol, on the surface of cellulose/NaOH/water gels, for 24 h (Figure 1). For a complete cellulose coagulation, the samples were then placed in large amount of the same non-solvent which was regularly exchanged (5 times); for example, the concentration of water after exchange with ethanol was below 0.005 % considering ethanol used does not contain water. Samples of coagulated cellulose with water in the pores are named “hydrogels” and with ethanol “alcogels” (Figure 1). To

have more information on the impact of the non-solvent used during solvent exchange, samples that were coagulated in water were placed in ethanol (to be dried with supercritical CO_2 or under low vacuum by evaporation,) and sample coagulated in ethanol were placed in water (to be dried under low vacuum by evaporation), see Figure 1.

Drug loading

The hydrogels and alcogels were immersed in 200 mL of theophylline dissolved at 2.5 g/L in water or in ethanol, respectively. This concentration was selected to have fully dissolved theophylline on one hand, and not too low drug concentration to be measurable during the study of release on the other hand[22,23]. Theophylline was selected as a model of small polar drugs; it has the advantages to be both soluble in water and ethanol and not soluble in supercritical CO_2. The diffusion of theophylline took place for 48 h at 20 °C under 200 rpm leading to cellulose sample loaded with the drug prior drying. To test the duration needed for theophylline to diffuse into cellulose sample, loading efficiency (see eq. 1 below) was measured after 24, 48 and 96 h, and was found to be completed after 48 h.

The loading efficiency of hydrogels and alcogels (*Loading efficiency "gel"*) was determined as follows: after loading, samples were crushed using mortar and pestle, 100 mL of deionized water was added, the dispersion was left under vigorous stirring for 48 h and sonicated for 30 min to fully extract theophylline. The dispersion was then filtered to remove cellulose particles and drug concentration was determined using spectrophotometry (see Section "Analysis of drug release"):

$$\textit{Loading efficiency « gel », \%} = \frac{m_{drug,\ gel}}{m_{theor}} \times 100 \qquad (1)$$

where $m_{drug,\ gel}$ is theophylline dose in alcogel or hydrogel and m_{theor} is the calculated drug dose supposing drug free diffusion between the bath and cellulose sample and no interactions between

theophylline and cellulose. As the volume of cellulose alcogel or hydrogel was 100 times smaller than the volume of the loading bath, the dilution of the loading bath by ethanol or water contained in alcogel or hydrogel was negligible within the experimental errors, and theophylline theoretical concentration inside the "gel" was considered to be 2.5 g/L.

Drying

Samples were dried using the following pathways (Figure 1):

1) by evaporation of non-solvent (water or ethanol) in the oven at 50°C under low vacuum, 5 kPa, until constant mass, resulting in "xerogels".

2) with supercritical CO_2 (sc CO_2) using procedure reported elsewhere[24], resulting in "aerogels". Alcogels were placed in tea bags and put in a 1 L autoclave (PERSEE, Mines Paris); the samples were covered by ethanol to avoid drying during system pressurization. The autoclave was then pressurized at 5 MPa, 37°C and the excess ethanol drained. The autoclave was then pressurized at 8 MPa to reach supercritical condition of carbon dioxide and the samples were dynamically washed with sc CO_2 for 4 h with an output of 5 kg_{CO2}/h. The depressurization was carried out at a rate of 0.5 MPa/h.

After reaching room temperature, all dry samples were collected and stored in a desiccator containing silica to avoid water uptake due to the ambient humidity. The preparation conditions and samples names are summarized in Table 1.

Table 1. Summary and nomenclature of the prepared samples: the first figure corresponds to cellulose concentration in solution, “E” and “H” to the non-solvent, ethanol (EtOH) or H_2O, respectively (EH or HE correspond to samples which underwent two non-solvent exchanges, see Figure 1), the last letter represents the drying technique: A stand for aerogel and X for xerogel.

Cellulose concentration (wt%)	First non-solvent	Non-solvent of drying	Drying technique	Sample name
3	Ethanol	Ethanol	Sc CO_2	3EA
5				5EA
3			Evaporation	3EX
5				5EX
3		H_2O	Evaporation	3EHX
5				5EHX
3	H_2O	H_2O	Evaporation	3HX
5				5HX
3		Ethanol	Sc CO_2	3HEA
5				5HEA
3			Evaporation	3HEX
5				5HEX

2.2.5. Material characterization

Volume shrinkage was calculated by measuring the dimensions of the disk-shaped samples using calliper (± 10 µm):

$$Shrinkage, \% = \frac{V_i - V_f}{V_i} \times 100 \quad (2)$$

where V_i corresponds to the initial volume (before solvent exchange or drying) and V_f to the final volume (after solvent exchange or drying).

The bulk density ρ_{bulk} of dry materials was calculated using equation 3:

$$\rho_{bulk} = \frac{m}{V_{dry}} \quad (3)$$

where m is the weight of the dry sample measured with high-precision balance, and V_{dry} obtained as mentioned above. Material porosity was calculated from bulk and skeletal (ρ_{sk}) density as follows:

$$P, \% = \left(1 - \frac{\rho_{bulk}}{\rho_{sk}}\right) \times 100 \quad (4)$$

with cellulose skeletal density taken as 1.5 g/cm^3.

Specific surface area (SSA) was determined by nitrogen adsorption with ASAP2020 (Micromeritics) using Brunauer-Emmet-Teller (BET) method. Prior measurement, samples were degassed under vacuum (1 Pa) at 70 °C for 10 hours.

Morphology of porous cellulose materials were analysed using Scanning Electron Microscope (SEM) MAIA (Tescan) equipped with Field Electron Gun. The samples were broken, a thin slice cut and placed on sample holder using carbon suspension. Sample cross-section was coated with 14 nm platinum layer using Q150T Quorum metallizer. Samples were analysed with an acceleration voltage of 3 kV.

X-ray diffraction measurements were carried using XPERT-PRO diffractometer (PANalytical) with a current of 30 mA, voltage of 45 kV using copper anode (λ = 1.54040 Å) over the 2θ range

5° - 60° with 0.08° step. Dried samples were crushed using mortar and pestle, the obtained powder was placed on to a zero-background silicon sample holder.

Analysis of drug release

The concentration of theophylline was recorded using Scanning Spectrophotometer UV-1800 UV/Visible (Shimadzu). First, the absorbance spectra and calibration dependences of theophylline absorbance at 271 nm[25] as a function of concentration were obtained (Figure S2). Molar extinction coefficient was estimated to be 10521 $L.mol^{-1}cm^{-1}$.

The loading efficiency of dry samples, *"loading efficiency dry"*, is defined as the ratio of theophylline dose in the dry cellulose $m_{drug,\ dry}$ and the theoretical theophylline dose m_{theor} calculated supposing drug free diffusion between the loading bath and cellulose sample and no interactions between theophylline and cellulose

$$Loading\ efficiency\ "dry",\ \% = \frac{m_{drug,\ dry}}{m_{theor}} \times 100 \qquad (5)$$

$m_{drug,\ dry}$ was the value obtained at the end of release experiment as no theophylline remained in cellulose (within the experimental errors), checked by crashing the sample and measuring theophylline concentration as described in the Section "Drug loading".

The kinetics of theophylline release was studied as follows. A drug-loaded dry sample was placed in stainless steel tee basket and immersed in 600 mL (sink conditions) of simulated gastric fluid (SGF) (HCl aqueous solution, pH = 1) for one hour, and then in 600 mL of simulated intestinal fluid (SIF) (KH_2PO_4 0.05 M aqueous solution, pH adjusted to 6.8 using NaOH) for the next 24 h, all at 37 °C and 100 rpm, to simulate the oral delivery of theophylline. The released fraction of theophylline $\frac{M(t)}{M}$ was analysed as a function of time *t*, where *M(t)* is the amount of theophylline

released at time *t*, and *M* is theophylline concentration at the end of release. For each sample type, the release was performed at least 3 times, and an average was calculated.

The volume changes of the dry materials after immersion in the release media were assessed by measuring sample volume with a calliper, and the volume shrinkage or swelling was calculated using Equation 1.

RESULTS AND DISCUSSION

Properties of neat cellulose materials

The photos of the representative samples are shown in Figure 2, and sample shrinkage during all processing steps in Figure 3. All samples underwent total shrinkage equal or higher than 50 vol% (eq. 2), as reported elsewhere[17]. Drying with sc CO_2 leads to lower total shrinkage compared to evaporative drying (Figure 3). In the latter case, shrinkage strongly depends on the type and sequence of non-solvents during solvent/non-solvent exchange (Figure 1). The xerogels coagulated in ethanol and dried from ethanol (samples 3EX and 5EX, Figure 2) have a similar aspect as aerogels while all other xerogels (cellulose dried from water: 3HX, 5HX, 3EHX and 5EHX, Figure 2) or coagulated in water as the first non-solvent (3HEX and 5HEX), undergo a significant shrinkage. Xerogels dried from water exhibit slight translucency.

Figure 2. Photos of the dry cellulose materials, aerogels (first row) and xerogels (second and third row). The scale is the same for all samples

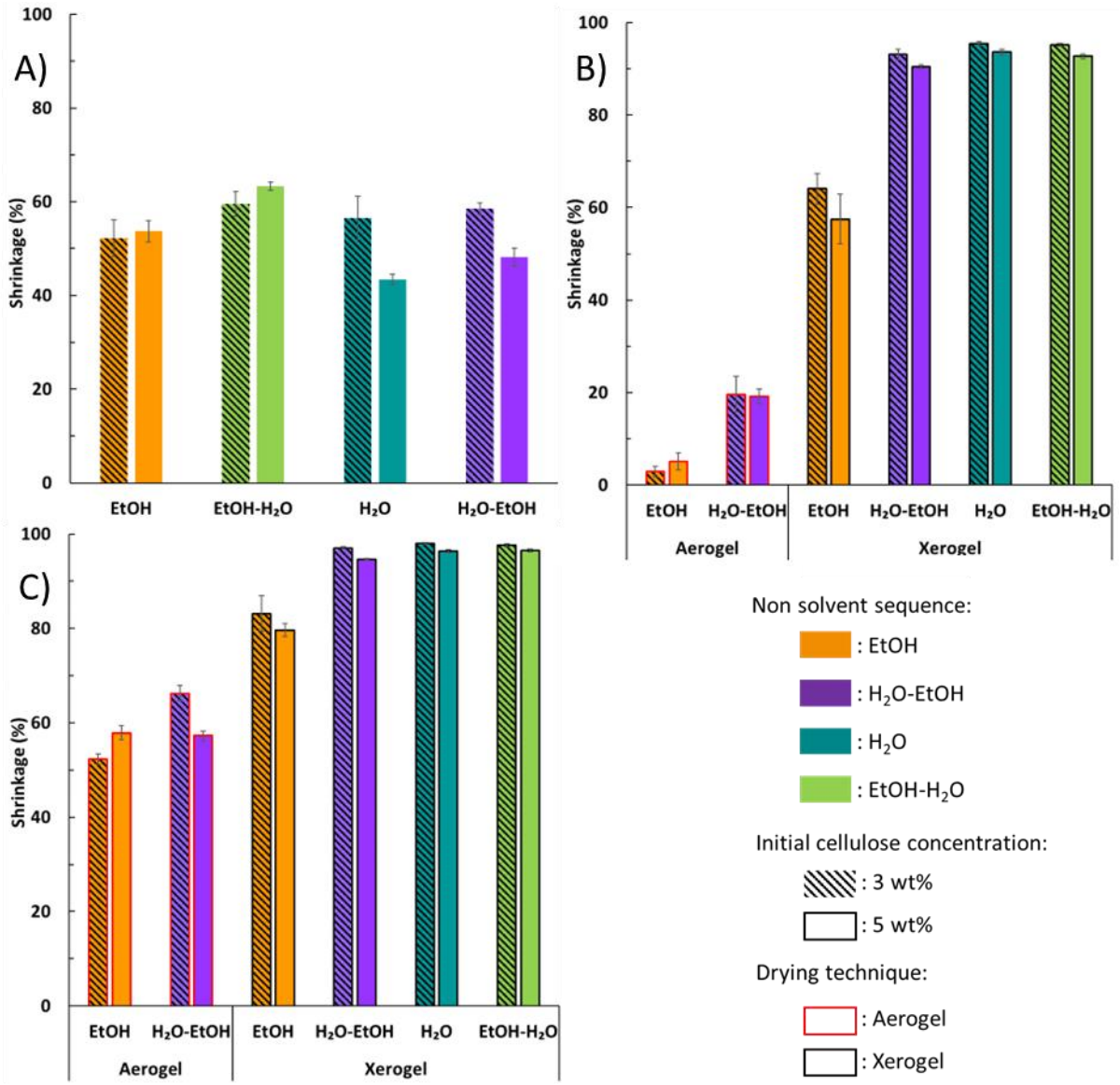

Figure 3. Shrinkage during the preparation of cellulose aerogels and xerogels: A) during solvent exchange, B) during drying and C) total shrinkage from gel to dry material

The replacement of solvent by non-solvent leads to cellulose chains aggregation, formation of a network of coagulated polymer, and sample macroscopic shrinkage within 45 - 60 % (Figure 3A). Similar results have been reported for various bio-aerogels[26–29]. While polymer chains tend to collapse in a non-solvent due to favourable polymer-polymer interactions, as known for synthetic

linear flexible polymers, cellulose is not shrinking much, most probably because of chain rigidity. When ethanol is used as the first non-solvent, no impact of cellulose concentration in the initial solution on the shrinkage (52 - 54%) was recorded within the experimental errors (Figure 3A). When water was used as the first non-solvent, gels with lower concentrated cellulose solutions shrink more (55 – 58%) than gels with higher concentration of cellulose (45 – 48%) (Figure 3A). The use of non-solvent with lower dielectric constant tends to lead to higher shrinkage for polysaccharides gels[26]. Lower shrinkage for higher-concentrated cellulose sample can be attributed to the higher mechanical properties of the gel, leading to better "resistance" during solvent exchange[18,26,30,31]. When cellulose undergoes two successive exchanges in different non-solvents, an additional small shrinkage during the second exchange was observed (Figure 3A). This phenomenon is reproducible and observed for all cases (Figure 3A): exchange of ethanol by water leads to 7 - 10% additional shrinkage, while the exchange of water by ethanol leads to lower additional shrinkage of 0 - 5%.

Shrinkage during drying is shown in Figure 3B. The most extensive shrinkage occurs during evaporative drying which can be explained, in majority, by the capillary pressure. It is defined, for cylindrical pores, by Young-Laplace equation:

$$P = \frac{2\gamma}{r_m} = \frac{2\gamma cos\theta}{r_p} \quad (7)$$

where γ is the surface tension between the vapor and the liquid, r_m the radius of the meniscus curvature, θ the contact angle between solid and liquid and r_p the pore radius. Other parameters, not counted in the capillary pressure, also influence cellulose shrinkage. For example, some shrinkage occurs during supercritical drying despite that no meniscus (and thus no capillary pressure) is developed in the supercritical state (Figure 3B). This shrinkage occurs due to a large difference in the polarity of cellulose and CO_2.

An important parameter influencing shrinkage is the surface chemistry of pore walls, which for cellulose can be hydrophilic or hydrophobic[32–34]. For example, it was demonstrated that the contact angle between cellophane-type film and water increases with the decrease of both cellulose crystallinity and planar orientation index f(1-10), the plane $1\bar{1}0$ having high density of hydroxyl groups[33]. When cellulose was dissolved in LiCl/dimethylacetamide and coagulated in methanol, the contact angle between amorphous cellulose and water was two-to-three times higher than that obtained for crystalline cellulose. Low-crystallinity materials were obtained for cellulose aerogels and xerogels dissolved in NaOH/water and coagulated in ethanol[35]. In case of 3D cellulose objects, the first coagulation fluid determines pore walls hydrophilicity, thus influencing further shrinkage. For example, for aerogels 3HEA and 5HEA, shrinkage during supercritical drying in a highly non-polar CO_2 was greater than that for the counterparts obtained when ethanol was the first coagulation bath (3EA and 5EA). For evaporative drying, higher affinity of cellulose to water compared to ethanol undoubtfully induces higher capillary pressure and thus higher shrinkage during evaporation from water compared to evaporation from ethanol.

Drying by evaporation of water induces higher shrinkage than that from ethanol also due to the difference in the surface tension of evaporating liquid, water vs ethanol (γ_{water} = 72.0 $mN.m^{-1}$ and $\gamma_{ethanol}$ = 21.82 $mN.m^{-1}$, at 298 K [36]): samples 3HX, 5HX, 3EHX and 5EHX exhibit extensive shrinkage during drying, 95 - 96% for 3 wt% cellulose solutions and 92 -94% for 5 wt% solutions vs 64% and 57% for 3EX and 5EX, respectively.

Still capillary pressure does not explain all the differences in shrinkages. For example, for the same evaporating non-solvent, higher polymer concentration leads to increased network mechanical properties resulting in a better resistance to capillary pressure: evaporative drying from hydrogels and alcogels made from 5% cellulose solutions lead to a slightly lower shrinkage compared to that from 3% cellulose solutions (Figure 3B). Another example shows again the

influence of the first non-solvent: for the same cellulose concentration and evaporating non-solvent, ethanol, shrinkage during drying is much lower when cellulose was coagulated in ethanol and dried from ethanol (around 60%) compared to the case when cellulose was coagulated in water and dried from ethanol (around 90%) (Figure 3B). The reason will be discussed below together with the analysis of sample morphology.

Figure 3C shows the total shrinkage during the whole preparation process which is a cumulated value for shrinkage during solvent/non-solvent exchange and drying. For aerogels the total shrinkage is 50 - 65 %, for xerogels around 80 % when coagulated and dried from ethanol, similar to the results reported in [37], and 90 – 98% for all other xerogels.

The bulk density of all materials is shown in Figure 4A; horizontal lines correspond to densities calculated for a hypothetical case of no shrinkage. Aerogels possess the lowest density, as expected, around 0.10 – 0.15 g/cm^3. Samples obtained from cellulose coagulated in ethanol and dried by evaporation from ethanol also possess low density, around 0.20 – 0.25 g/cm^3. In both cases of low-density materials higher polymer concentration in the initial solution leads to higher bulk density, as reported for numerous bio-aerogels[28,31,38,39]. All the other xerogels obtained either via coagulation in water or dried from water have high density, above 0.8 g/cm^3, up to 1.2 g/cm^3, close to cellulose skeletal density (1.5 g/cm^3). Within this family of dry materials, the samples coagulated in water and dried from ethanol possess the lowest density, 0.81 – 0.84 g/cm^3. In the case of cellulose dried from ethanol by evaporation, the first non-solvent used during coagulation has a strong impact on the final shrinkage: samples that were first coagulated in water exhibit density almost 4 times higher than the one coagulated in ethanol and dried in ethanol.

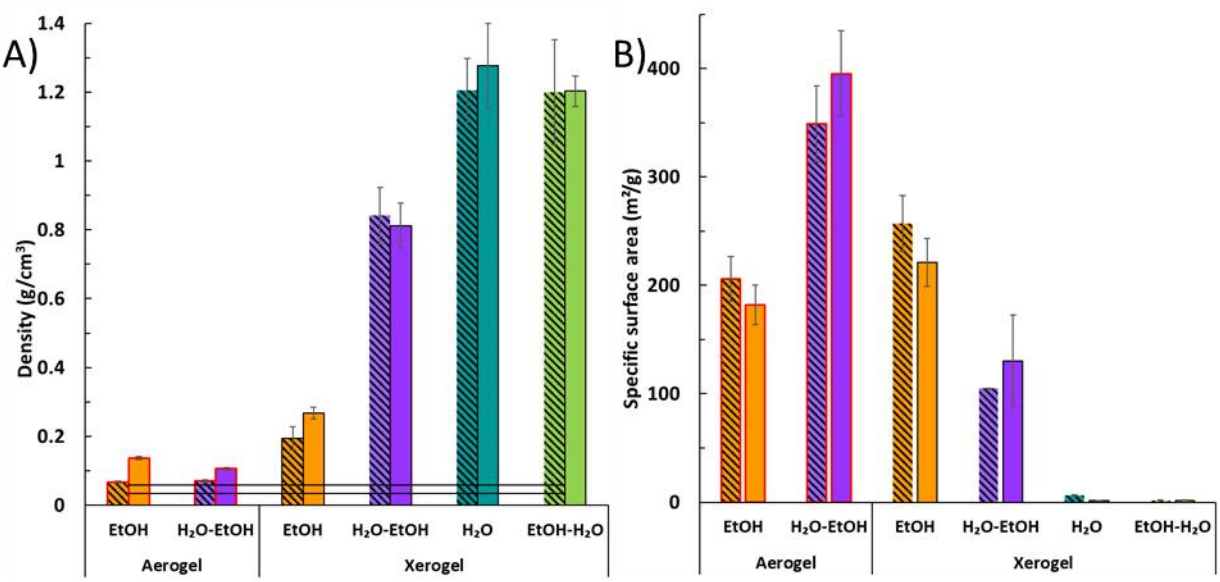

Figure 4. (A) Density of aerogels and xerogels; two solid lines correspond to the theoretical density of no shrinkage during processing (0.035 and 0.058 g/cm^3 for materials from cellulose solutions of 3 and 5 wt%, respectively); (B) specific surface area of dry cellulose materials. Symbols and notations are the same as in Figure 3.

Figure 4B summarizes the specific surface area (SSA) obtained for all materials. It strongly depends on the preparation method and varies from a few to 400 m²/g. Cellulose dried by evaporation of water exhibits negligible SSA due to pore collapse during drying. In contrast, aerogels show high SSA, ranging from 180-200 m²/g (coagulated in ethanol: 3EA and 5EA) to 350-400 m²/g (coagulated in water, then replaced by ethanol: 3HEA and 5HEA). Xerogels obtained via coagulation in ethanol and dried from ethanol possess SSA of 220-260 m²/g, which is even higher than that of the corresponding aerogels[35]. Xerogels formed by cellulose coagulation in water, followed by exchange to ethanol and subsequent drying from ethanol, exhibit lower SSA, 105 - 130 m²/g.

The results obtained on materials' density (Figure 4A) and specific surface area (Figure 4B), combined with morphology analysed by SEM (Figure 5 and Figure S3), demonstrate that not only the type of drying (in supercritical conditions vs evaporation), but also the type of the first non-solvent determines the properties of cellulose porous material[34,40]. Upon the addition of a non-solvent, cellulose/cellulose interactions are favoured, and phase separation occurs. Our first hypothesis is that chains' assembly, and thus the thickness of pore walls, depend on polymer affinity to the non-solvent. Upon the addition of water, a fine network of cellulose fibrils is formed. This network is well preserved during the exchange of water to ethanol and $scCO_2$ drying, resulting in high SSA, 350 – 400 m^2/g, and morphology with large number of mesopores and thin pore walls (Figure 5, sample 5HEA). On the opposite, when cellulose/8%NaOH/water gels are coagulated in ethanol, cellulose chains tend to decrease the contact with this non-solvent, assembling into thicker fibrils, and forming a rather hydrophobic surface. The as-obtained aerogels possess surface area twice lower (180 – 200 m^2/g) than that of aerogels of which the first coagulation medium was water, with large number of macropores (Figure 5, sample 5EA). Our second hypothesis is that thick pore walls of cellulose coagulated in ethanol help resisting capillary pressure during evaporative drying from ethanol, resulting in xerogels with surface area of 257 and 221 m^2/g and density of 0.27 and 0.19 g/cm^3 for 5EX and 3EX, respectively (see morphology of sample 5EX on Figure 5 and Figure S3, respectively). On the opposite, when the first coagulation bath is water, further exchanged to ethanol and drying performed from ethanol by evaporation, the network of fine fibrils in hydrogel does not withstand the capillary pressure during evaporative drying, resulting in xerogels of rather high density (0.8 g/cm^3) and with a certain number of mesopores, but much less than in 3EX and 5EX counterparts, indicating partial pore closure (SSA from 105 to 130 m^2/g for 3HEX and 5HEX m^2/g, respectively). Figure 5 confirmed the absence of visible porosity in cellulose materials dried from water. Finally, other factors, such as formation of

"spacers" when cellulose/NaOH/water gel is coagulated in ethanol and dried from ethanol, prevents chains aggregation and network collapse during drying. These "spacers" can be either remaining sodium trapped in-between cellulose chains and/or carbonate bridges[35,41].

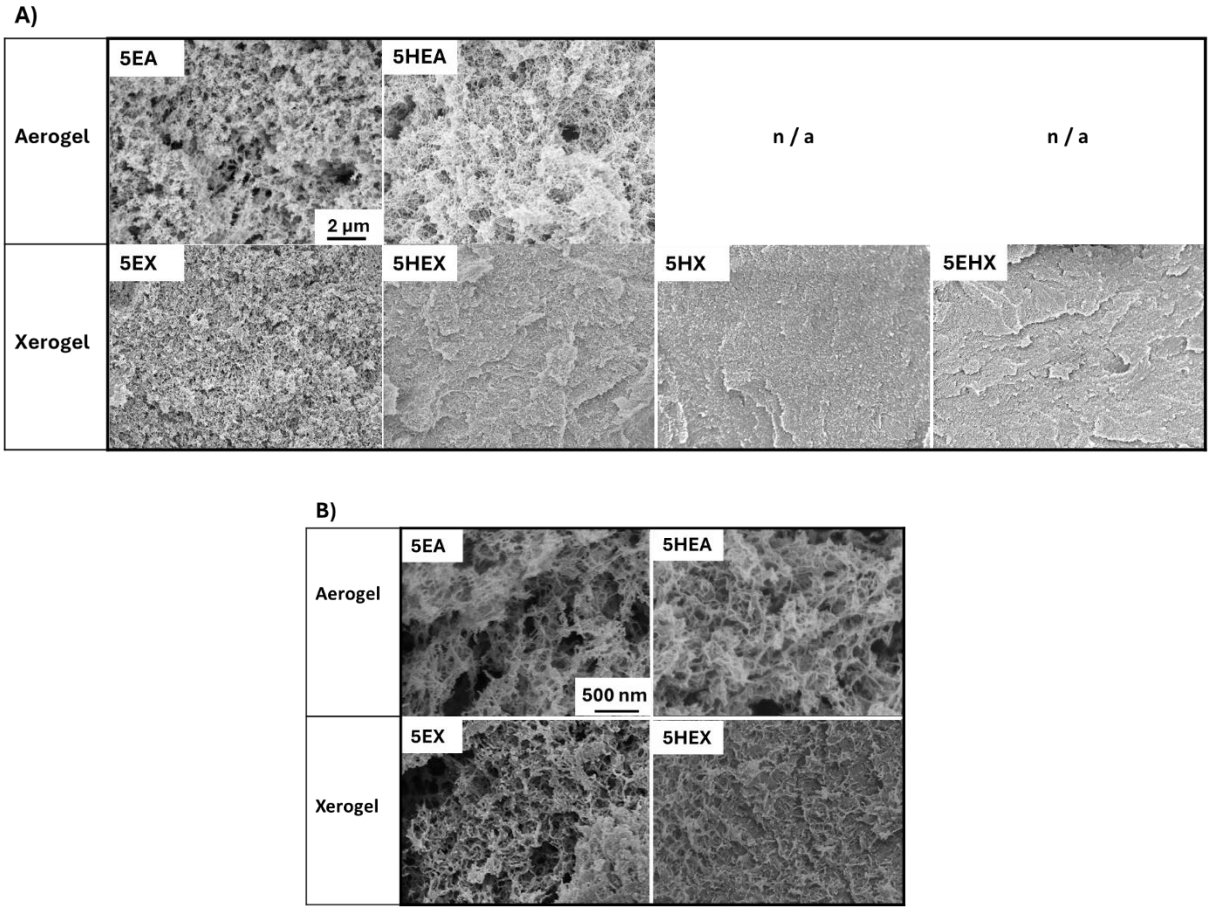

Figure 5. Morphology of cellulose materials at the scale of 2 µm (A) and 500 nm (B). All samples were made from 5%cellulose/8%NaOH/water solutions.

In general, supercritical drying can be regarded as another non-solvent exchange using an apolar non-solvent, which may lead to some degree of cellulose aggregation. While rearrangements could occur during supercritical drying, they appear to be minimal in our case (Figure 3C), and the

morphology of the aerogels can be considered as approximation of the coagulated cellulose morphology. It is also important to note that the observations given above are relevant to this specific solvent system. As well as other process parameter, the choice of solvent also plays a crucial role in the final morphology of the aerogel and in xerogel properties[35,42,43].

Theophylline-loaded cellulose hydrogel, alcogel, aerogel and xerogel

All materials presented in the section above are without the drug. When cellulose was impregnated with theophylline (see Methods section), the properties of the loaded materials were identical to those of neat cellulose, within the experimental errors. We remind that theophylline was loaded by diffusion by placing the sample in the theophylline/ethanol or theophylline/water solution before drying (Figure 1). The concentration of theophylline in the loading bath was the same in all cases.

The loading efficiency of cellulose samples before drying (eq. 1) (hydrogels and alcogels, see Figure 1) and of dry samples (eq.5) is presented in Table 2. First let us consider non-dried samples, i.e. hydrogels and alcogels. When theophylline was loaded from water in cellulose hydrogel with water being the only coagulation liquid, the loading efficiency was 100%, as expected. Osmotic equilibrium between the loading bath and the hydrogel was reached: no drug adsorption occurred. Interestingly, this was not the case when theophylline was loaded from ethanol with ethanol being the only coagulation liquid: the loading efficiency of alcogels was superior to 200% (Table 2), i.e. theophylline was adsorbed by cellulose. A similar result was obtained for theophylline adsorbed by starch from ethanol[44]. This behaviour can be attributed to the difference in surface chemistry of cellulose pore walls which depends on the non-solvent used. Crystal plane orientation defines cellulose surface hydrophilic/hydrophobic balance and guides adsorption properties[33,45]. Surface

chemistry, combined with different affinity of theophylline towards water and ethanol, explains the obtained results. When the loading liquid was not the same as the one used for the first coagulation bath (EH and HE samples), the obtained loading efficiency was slightly higher than 100%, between 114 and 121% (Table 2).

Next, we consider the case when cellulose alcogels and hydrogels were dried by evaporation in low vacuum (i.e. xerogels). The loading efficiency of xerogels followed the trend of the corresponding "wet" samples, as expected (Table 2): around 100% when only water was used for coagulation and evaporation, above 200 % for xerogels dried from ethanol (coagulation in ethanol only), and 110 – 120 % for H_2O → ethanol and ethanol → H_2O coagulation sequences.

Finally, for both types of aerogels the loading efficiency was lower than 100%, around 60 – 80%. Despite the non-solubility of theophylline in CO_2, the drug could have been washed out during the first steps of ethanol-CO_2 mixing as theophylline may still be partly soluble in the ethanol/CO_2 mixture. The dynamic step during CO_2 drying (see Methods) could also have led to drug partial wash-out, as reported previously for theophylline-loaded pectin aerogels[27].

Table 2. The loading efficiency of hydrogels (loading from water), alcogels (loading from ethanol), xerogels and aerogels; cellulose concentration in the initial solutions was 5%

Non-solvent sequence	H_2O only (H)	Ethanol only (E)	H_2O → ethanol (HE)	Ethanol → H_2O (EH)
Hydrogel or alcogel	104 ± 5	210 ± 87	121 ± 2	114 ± 2
Xerogel	100 ± 8 (HX)	274 ± 31 (EX)	115 ± 7 (HEX)	89 ± 25 (EHX)
Aerogel	n/a	86 ± 31 (EA)	62 ± 39 (HEA)	n/a

3.3. Release kinetics of theophylline from cellulose aerogels and xerogels

Numerous parameters can influence drug release kinetics, including drug crystallinity and solubility, polymer swelling/relaxation, drug dispersion inside release device, material morphology (open or closed porosity), carrier volume change, and polymer-drug interactions. The kinetics of drug dissolution depends on the form in which the drug is present inside the device. Theophylline can be in amorphous or crystalline state with different polymorphs[46,47]. To check if theophylline is crystalline or amorphous inside loaded cellulose materials, XRD was performed on samples made from 3 wt% cellulose solution. Since the drying method may influence theophylline crystallization, XRD patterns were recorded for samples dried with supercritical CO_2 and by evaporation of ethanol or water. The obtained XRD spectra are shown in Figure S4 together with the one of neat theophylline crystals (mixture of crystalline anhydrous theophylline and theophylline monohydrate). The patterns of loaded samples show no detectable traces of crystalline theophylline whatever is the drying, indicating the presence of amorphous theophylline inside all cellulose materials.

As the release of theophylline was performed in the media of different pH (see Methods), the influence of the type of release medium, SGF and SIF, on the release kinetics was first checked. An example of theophylline release in SGF alone and in SIF alone from aerogels 3HEA is shown in Figure S5. No influence of the type of release medium on release kinetics from cellulose materials was recorded as the curves of release in SIF and SGF superposed. pH of the release media does not affect cellulose as it is a neutral polymer, opposite to pectin[27]. The dissolution of neat theophylline in SGF is also shown for comparison in Figure S5: it is immediate, with 95% of theophylline is dissolved within the first minute. All theophylline was released from all tested materials (within experimental errors).

To analyse the release kinetics, the behaviour of the delivery device itself should be monitored as it may swell, shrink, erode and/or dissolve. As expected, no cellulose sample dissolved, and no erosion was recorded. All materials absorb water but depending on the type of non-solvent used for coagulation and on sample porosity, cellulose carriers were swelling or shrinking, reaching equilibrium with different kinetics (Table 3). For example, all highly porous celluloses, such as all aerogels (3EA, 5EA, 3HEA, 5HEA) and xerogels obtained by drying from ethanol (3EX, 5HX), show fast (within first 10 min) volume shrinkage, less than around 30 – 35% (Table 3). This rapid shrinkage corresponds to the capillary pressure exerted on the pore walls during the wetting of the system, leading to the collapse of small pores (all samples are of high specific surface area). Similar volume shrinkage in release medium has been reported for chitosan aerogels[48]. The timescale of a few minutes is consistent with the kinetics of fluid penetration into a porous system as described by the Washburn equation[49]. After this fast shrinkage, the volume of the initially highly porous samples does not change anymore during theophylline release.

Table 3. Cellulose aerogels and xerogels' volume swelling (+ ΔV) or shrinking (- ΔV) (eq.6) in the release medium; mean values of porosity and specific surface area (taken from Figure 3b) are given to help correlating with material properties, and "fast" corresponds to volume change within 10 min.

Sample	Porosity, %	Specific surface area, m^2/h	ΔV, %	Remark
3EA	96	206	- 25 / - 35	fast shrinking
5EA	92	182	- 25 / - 35	fast shrinking
3EX	76	257	- 30 / - 35	fast shrinking

5EX	75	221	- 30	fast shrinking
3EHX	23	2	+ 50	fast swelling up to 10% followed by slow swelling
5EHX	22	2	+ 70 / + 80	fast swelling up to 20% followed by slow swelling
3HX	25	6	+ 70 / +80	fast swelling up to 20% followed by slow swelling
5HX	16	1	+ 60 / + 70	fast swelling up to 10% followed by slow swelling
3HEA	95	349	- 10 / - 15	fast shrinking
5HEA	93	395	- 10 / - 15	fast shrinking
3HEX	46	105	+ 30 / + 35	slow swelling
5HEX	48	130	+ 30 / + 35	slow swelling

Xerogels dried from water (3EHX, 5EHX, 3HX and 5HX) are of very low porosity and negligible surface area, and they continuously and slowly swell up to + 70 / +80% of their volume (Table 3). This slow swelling corresponds to penetration of water into cellulose sample. Finally, xerogels obtained by coagulation of cellulose first in water, water replaced by ethanol and dried from ethanol, show low slow swelling (3HEX and 5HEX, Table 3). These samples are of porosity in-between aerogels and water-dried xerogels, and of surface area around 100 m^2/g. Potential shrinkage due to the collapse of certain number of small pores is counterbalanced by swelling due to cellulose affinity to water, resulting of practically no volume change. It should be noted that even for highly porous samples exhibiting shrinkage during the release process, it is anticipated

that water induces swelling of the cellulose pore walls. However, this swelling occurs within the water-filled spaces of the pores[50–52].

As our cellulose materials show different volume change when immersed in the release medium, the kinetics of theophylline release is presented by regrouping samples with the same behaviour, i.e. those that are shrinking and those that are swelling. Let us first consider porous samples (porosity > 70%, Table 3) that are shrinking. To compare the release kinetics from samples of different thickness (see Figure 2), time was normalized by the square of half-thickness l^2 as it is usually done for diffusion-controlled processes in porous materials. As sample volume decreased within the first 10 min of release, l was taken as the half-thickness of the sample at the end of the release. No theoretical approaches established for the analysis of release kinetics were applied to the results obtained as the aspect ratio (sample disk thickness to diameter ratio) was too high, around 0.24 – 0.34 (Figure S6), and also because in several cases the amount of data within 60% of cumulated release was insufficient due to the rapid release in the first minutes.

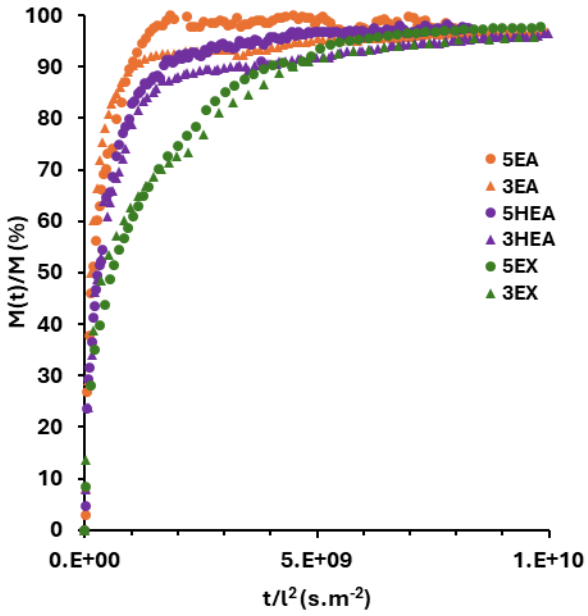

Figure 6. Theophylline release kinetics from porous cellulose materials (porosity above 70%), aerogels and xerogels, that are shrinking within the first 10 min. For more details and samples nomenclature see Table 3.

Figure 6 shows that release kinetics from samples of similar high porosity (above 90%), i.e. all aerogels (3HEA, 5HEA, 3EA and 5EA), is very similar; 85 – 90% of the drug is released at t/l^2 around 1.5×10^{-9} $s.m^{-2}$. The release is slower from porous xerogels which are of lower porosity (75 – 76%). In all cases shown in Figure 6, 50% of the drug is released within t/l^2 around 1.0×10^{9} ($s.m^{-2}$). An example of the release kinetics during the first few hours for 3EA sample is shown in Figure S7. A similar rather fast release of the 50 - 60% of model compounds was reported for cellulose aerogels made from cellulose dissolved in 60% zinc chloride and coagulated in isopropanol[13] and for bacterial cellulose aerogels[11]. When immersed in the release medium, the drug that is located on and near sample surface dissolves leading to a fast release of 50 – 60% of loaded theophylline. Another reason of the fast release of the first 50% of drug is the fast shrinkage upon immersion in the release medium (Table 3). Such fast initial release may be, on one hand, undesirable, or, on the other hand, advantageous for quickly achieving certain therapeutic efficiency[53]. As far as cellulose does not dissolve or erode, the main parameter controlling the release is material porosity (or density). Among the samples shown in Figure 6, the release from porous cellulose xerogels (3EX and 5EX) is more sustained due to lower porosity, as reported in the literature for other drug delivery devices[54,55].

The cumulative release of theophylline from slowly swelling cellulose materials of low porosity, below 50%, is presented in Figure 7a as a function of time for the samples of the same thickness. All samples show a fast release of the 50% of the drug, as in the cases of highly porous materials

(Figure 6). The difference in release kinetics between samples of similar porosity, 5HX and 5EHX, may be explained by different surface to volume ratio (Figure S6), but, overall, higher material porosity, faster release, as expected. The most sustained release was from non-porous samples (xerogels obtained from cellulose hydrogel dried from water by evaporation) with total duration around 24 h. In all cases studied, no correlation was found between the material's specific surface area and the release kinetics; porosity is the dominating factor in the absence of strong interactions between the drug and the carrier.

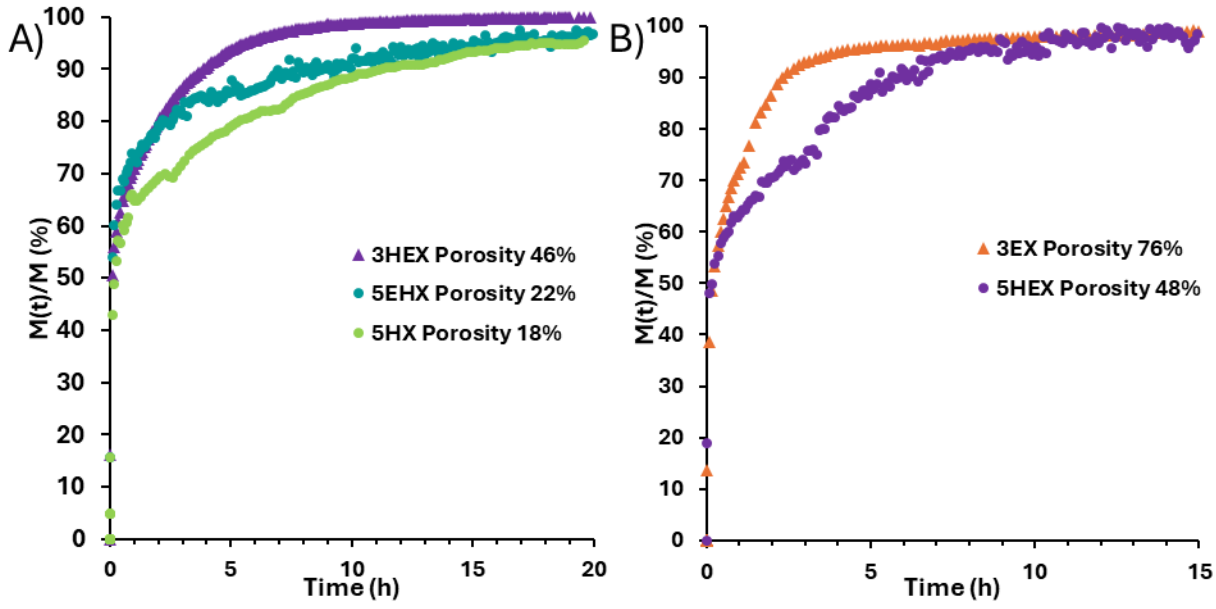

Figure 7. Comparison of release kinetics from samples of the same thickness: 5HX, 5EHX and 3HEX ($2l$ = 2.6; 2.7 mm) (A), and 5HEX and 3EX ($2l$ = 3.3 mm) (B). Error bars are not shown here to avoid figures' overloading; the examples with errors are shown in Figure S8.

A comparison of the release kinetics from xerogels of the same thickness, both dried from ethanol, fast-shrinking highly-porous xerogel (3EX) and slow-swelling xerogel (first coagulation fluid water, 5HEX), is shown in Figure 7B. As expected, the fastest release is from highly porous

xerogel, within 5 h, vs 10 h for 5HEX. This result confirms the strong influence of material porosity.

The release kinetics from non-dissolving and non-eroding devices should be primarily governed by drug diffusion. As demonstrated above, depending on the processing pathway, a material obtained can be with open porosity or pores may close during drying. In the former case theophylline is deposited on pore walls, and in the latter theophylline is trapped inside. In this context, two diffusion mechanisms should be considered: the diffusion of theophylline through aqueous medium-filled pores and channels, and its diffusion through cellulose pore walls. In the latter case cellulose swelling should be considered allowing diffusion of theophylline through pore walls to reach the release medium-filled pores. The kinetics of drug release and sample volume evolution for each low-porosity xerogel is presented in Figure S9. It shows direct correlation between sample swelling and drug release kinetics.

CONCLUSIONS

Cellulose materials of various porosity and specific surface area were prepared from cellulose/8%NaOH/water solutions without any additive or crosslinker, by varying processing conditions: the type and order of non-solvent (water, ethanol) and drying technique, either drying with supercritical CO_2 (aerogels) or by evaporation under low vacuum (xerogels). When water was the first coagulation bath, aerogels were with twice higher specific surface area (350 - 400 m^2/g) compared to their counterparts obtained when the first coagulation bath was ethanol (180 – 210 m^2/g). When evaporation of ethanol was performed in low vacuum, aerogel-like xerogels were obtained if the first coagulation bath was ethanol (density 0.19 – 0.26 g/cm^3 and surface area 260 - 220 m^2/g) while if the first coagulation bath was water, material density was 0.8 – 0.85 g/cm^3 and surface area around 100 – 130 m^2/g.

The properties of the evaporating fluid do not explain all the differences in cellulose transformations during drying. When coagulated in ethanol, thicker fibrils (or pore walls) are formed, resulting in aerogels with lower surface area, but the network was resistant to capillary pressure during evaporative drying. The latter results in xerogels with aerogel-like properties. On the opposite, when cellulose is coagulated in water, the network of fine morphology results in aerogels with high surface area. However, this fine network cannot withstand the capillary pressure during evaporative drying, leading to structure collapse.

Cellulose hydrogels and alcogels were loaded with theophylline by diffusion. When the loading of theophylline was performed from ethanol solution into alcogel, adsorption of theophylline by cellulose was recorded. This suggests that surface chemistry plays a crucial role in the adsorption of theophylline on cellulose pore walls. All theophylline was, nevertheless, released from all aerogels and xerogels indicating no chemical bonding of the drug to cellulose. Drug release kinetics from the resulting dried materials in simulated gastrointestinal environment was evaluated.

The extensive number of variables makes the fine analysis of drug release kinetics a challenging task. In this study, the release kinetics was primarily driven by material porosity. Starting from the same initial cellulose/8% NaOH/water solution, theophylline release kinetics was significantly varied (total release from 5 to 20 hours) only by altering processing conditions. The processing of cellulose into aerogels and xerogels offers a broad range of possibilities for tuning porosity, surface properties, pore size, loading capacity and release kinetics.

SUPPORTING INFORMATION:

Figures: S1 (Determination of intrinsic viscosity of microcrystalline cellulose in 0.5 M cupraethylenediamine); S2 (Calibration dependence for the determination of molar extinction coefficient of theophylline by spectrophotometry); S3 (Morphology of cellulose materials made from

3%cellulose/8%NaOH/water solutions; the scale is the same for all images); S4 (XRD pattern of theophylline (2 allomorphs are present: theophylline monohydrate and anhydrous theophylline) and of dry cellulose samples containing theophylline); S5 (Dissolution kinetics of neat theophylline (green triangles) and release kinetics of theophylline from 3HA into simulated intestinal fluid (SIF) alone and into simulated gastric fluid (SGF) alone); S6 (Sample external surface to volume ratio (A) and aspect ratio (B)); S7 (Example of theophylline release kinetics from 3EA aerogel); S8 (Reproduction of Figure 7 with error bars) and S9 (Correlation between kinetics of theophylline release and cellulose sample swelling for low-porosity xerogels).

ACKNOWLEDGEMENTS:

The authors are thankful to Dr. Julien Jaxel (PERSEE, MINES Paris) for supercritical drying. The financial support was granted by Agence nationale de la recherche (ANR), project number ANR-21-CE43-0017-01 (Bio-gels).

REFERENCES

(1) Meng, Y.; Qiu, C.; Li, X.; McClements, D. J.; Sang, S.; Jiao, A.; Jin, Z. Polysaccharide-Based Nano-Delivery Systems for Encapsulation, Delivery, and pH-Responsive Release of Bioactive Ingredients. Crit Rev Food Sci Nutr. **2024**, 64 (1),187-201. DOI: 10.1080/10408398.2022.2105800.

(2) Kosaraju, S. L. Colon Targeted Delivery Systems: Review of Polysaccharides for Encapsulation and Delivery. *Crit Rev Food Sci Nutr. **2005**, 45 (4), 251-258*. DOI: 10.1080/10408690490478091.

(3) Alvarez-Lorenzo, C.; Concheiro, A. Smart Drug Release from Medical Devices. *J Pharmacol Exp Ther.* **2019**, *370* (3), 544–554. DOI: 10.1124/jpet.119.257220.

(4) Reier, G. E.; Shangraw, R. F. Microcrystalline Cellulose in Tableting. *Journal of Pharmaceutical Sciences* **1966**, *55* (5), 510–514. DOI: 10.1002/jps.2600550513.

(5) Colombo, P.; Sonvico, F.; Colombo, G.; Bettini, R. Novel Platforms for Oral Drug Delivery. *Pharm Res.* **2009**, *26* (3), 601–611. DOI: 10.1007/s11095-008-9803-0.

(6) Trache, D.; Hussin, M. H.; Hui Chuin, C. T.; Sabar, S.; Fazita, M. R. N.; Taiwo, O. F. A.; Hassan, T. M.; Haafiz, M. K. M. Microcrystalline Cellulose: Isolation, Characterization and Bio-Composites Application—A Review. Int J Biol Macromol. **2016**, *93*, 789–804. DOI: 10.1016/j.ijbiomac.2016.09.056.

(7) Yassin, S.; Goodwin, D. J.; Anderson, A.; Sibik, J.; Ian Wilson, D.; Gladden, L. F.; Axel Zeitler, J. The Disintegration Process in Microcrystalline Cellulose Based Tablets, Part 1: Influence of Temperature, Porosity and Superdisintegrants. *J Pharm Sci.* **2015**, *104* (10), 3440–3450. DOI: 10.1002/jps.24544.
(8) García-González, C. A.; Sosnik, A.; Kalmár, J.; De Marco, I.; Erkey, C.; Concheiro, A.; Alvarez-Lorenzo, C. Aerogels in Drug Delivery: From Design to Application. *J. Controlled Release* **2021**, *332*, 40–63. DOI: 10.1016/j.jconrel.2021.02.012.
(9) Ciolacu, D. E.; Nicu, R.; Ciolacu, F. Cellulose-Based Hydrogels as Sustained Drug-Delivery Systems. *Materials* **2020**, *13* (22), 5270. DOI: 10.3390/ma13225270.
(10) Salimi, S.; Sotudeh-Gharebagh, R.; Zarghami, R.; Chan, S. Y.; Yuen, K. H. Production of Nanocellulose and Its Applications in Drug Delivery: A Critical Review. *ACS Sustainable Chem. Eng.* **2019**, *7* (19), 15800–15827. DOI: 10.1021/acssuschemeng.9b02744.
(11) Haimer, E.; Wendland, M.; Schlufter, K.; Frankenfeld, K.; Miethe, P.; Potthast, A.; Rosenau, T.; Liebner, F. Loading of Bacterial Cellulose Aerogels with Bioactive Compounds by Antisolvent Precipitation with Supercritical Carbon Dioxide. *Macromol. Symp.* **2010**, *294* (2), 64–74. DOI: 10.1002/masy.201000008.
(12) Liu, Z.; Zhang, S.; He, B.; Wang, S.; Kong, F. Synthesis of Cellulose Aerogels as Promising Carriers for Drug Delivery: A Review. *Cellulose* **2021**, *28* (5), 2697–2714. DOI: 10.1007/s10570-021-03734-9.
(13) Rostamitabar, M.; Subrahmanyam, R.; Gurikov, P.; Seide, G.; Jockenhoevel, S.; Ghazanfari, S. Cellulose Aerogel Micro Fibers for Drug Delivery Applications. *Mater. Sci. Eng., C* **2021**, *127*, 112196. DOI: 10.1016/j.msec.2021.112196.
(14) Budtova, T.; Navard, P. Cellulose in NaOH–Water Based Solvents: A Review. *Cellulose* **2016**, *23* (1), 5–55. DOI: 10.1007/s10570-015-0779-8.
(15) Ciolacu, D.; Rudaz, C.; Vasilescu, M.; Budtova, T. Physically and Chemically Cross-Linked Cellulose Cryogels: Structure, Properties and Application for Controlled Release. *Carbohydr. Polym.* **2016**, *151*, 392–400. DOI: 10.1016/j.carbpol.2016.05.084.
(16) Groult, S.; Buwalda, S.; Budtova, T. Tuning Bio-Aerogel Properties for Controlling Drug Delivery. Part 2: Cellulose-Pectin Composite Aerogels. Biomater. Adv. **2022**, 212732. DOI: 10.1016/j.bioadv.2022.212732.
(17) Budtova, T. Cellulose II Aerogels: A Review. *Cellulose* **2019**, *26* (1), 81–121. DOI: 10.1007/s10570-018-2189-1.
(18) Gavillon, R.; Budtova, T. Aerocellulose: New Highly Porous Cellulose Prepared from Cellulose−NaOH Aqueous Solutions. *Biomacromolecules* **2008**, *9* (1), 269–277. DOI: 10.1021/bm700972k.
(19) Cai, J.; Kimura, S.; Wada, M.; Kuga, S.; Zhang, L. Cellulose Aerogels from Aqueous Alkali Hydroxide-Urea Solution. *ChemSusChem* **2008**, *1* (1–2), 149–154. DOI: 10.1002/cssc.200700039.
(20) Chin, S.-F.; Jimmy, F. B.; Pang, S.-C. Fabrication of Cellulose Aerogel from Sugarcane Bagasse as Drug Delivery Carriers. *J. Phys. Sci.* **2016**, *27* (3), 159–168. DOI: 10.21315/jps2016.27.3.10.
(21) Roy, C.; Budtova, T.; Navard, P. Rheological Properties and Gelation of Aqueous Cellulose−NaOH Solutions. *Biomacromolecules* **2003**, *4* (2), 259–264. DOI: 10.1021/bm020100s.
(22) Zhong, J.; Tang, N.; Asadzadeh, B.; Yan, W. Measurement and Correlation of Solubility of Theobromine, Theophylline, and Caffeine in Water and Organic Solvents at Various Temperatures. *J. Chem. Eng. Data* **2017**, *62* (9), 2570–2577. DOI: 10.1021/acs.jced.7b00065.

(23) Subra, P.; Laudani, C.-G.; Vega-González, A.; Reverchon, E. Precipitation and Phase Behavior of Theophylline in Solvent–Supercritical CO2 Mixtures. *J. Supercrit. Fluids* **2005**, *35* (2), 95–105. DOI: 10.1016/j.supflu.2004.12.010.
(24) Yu, S.; Budtova, T. Creating and Exploring Carboxymethyl Cellulose Aerogels as Drug Delivery Devices. *Carbohydr. Polym*. **2024**, *332*, 121925. DOI: 10.1016/j.carbpol.2024.121925.
(25) Grassi, M.; Colombo, I.; Lapasin, R. Experimental Determination of the Theophylline Diffusion Coefficient in Swollen Sodium-Alginate Membranes. *J. Controlled Release* **2001**, *76* (1), 93–105. DOI: 10.1016/S0168-3659(01)00424-2.
(26) Gurikov, P.; S. P., R.; Griffin, J. S.; Steiner, S. A.; Smirnova, I. 110th Anniversary: Solvent Exchange in the Processing of Biopolymer Aerogels: Current Status and Open Questions. *Ind. Eng. Chem. Res.* **2019**, *58* (40), 18590–18600. DOI: 10.1021/acs.iecr.9b02967.
(27) Groult, S.; Buwalda, S.; Budtova, T. Tuning Bio-Aerogel Properties for Controlling Theophylline Delivery. Part 1: Pectin Aerogels. *Mater. Sci. Eng., C* **2021**, *126*, 112148. DOI: 10.1016/j.msec.2021.112148.
(28) Chartier, C.; Buwalda, S.; Van Den Berghe, H.; Nottelet, B.; Budtova, T. Tuning the Properties of Porous Chitosan: Aerogels and Cryogels. *Int. J. Biol. Macromol.* **2022**, *202*, 215–223. DOI: 10.1016/j.ijbiomac.2022.01.042.
(29) Legay, L.; Budtova, T.; Buwalda, S. Hyaluronic Acid Aerogels Made Via Freeze–Thaw-Induced Gelation. *Biomacromolecules* **2023**, *24* (10), 4502–4509. DOI: 10.1021/acs.biomac.2c01518.
(30) Buchtová, N.; Budtova, T. Cellulose Aero-, Cryo- and Xerogels: Towards Understanding of Morphology Control. *Cellulose* **2016**, *23* (4), 2585–2595. DOI: 10.1007/s10570-016-0960-8.
(31) Innerlohinger, J.; Weber, H. K.; Kraft, G. Aerocellulose: Aerogels and Aerogel-like Materials Made from Cellulose. *Macromol. Symp.* **2006**, *244* (1), 126–135. DOI: 10.1002/masy.200651212.
(32) Lindman, B.; Medronho, B.; Alves, L.; Costa, C.; Edlund, H.; Norgren, M. The Relevance of Structural Features of Cellulose and Its Interactions to Dissolution, Regeneration, Gelation and Plasticization Phenomena. *Phys. Chem. Chem. Phys*. **2017**, *19* (35), 23704–23718. DOI: 10.1039/C7CP02409F.
(33) Yamane, C.; Aoyagi, T.; Ago, M.; Sato, K.; Okajima, K.; Takahashi, T. Two Different Surface Properties of Regenerated Cellulose Due to Structural Anisotropy. *Polym. J.* **2006**, *38* (8), 819–826. https://doi.org/10.1295/polymj.PJ2005187.
(34) Aiello, A.; Nguyen, H. G.; Stafford, C. M.; Woodcock, J. W. Impact of Coagulation Solvent Interactions on Porous Morphology Evolution in Cellulose Xerogels. *Carbohydr. Polym.* **2024**, *323*, 121454. DOI: 10.1016/j.carbpol.2023.121454.
(35) Druel, L.; Budtova, T. Aerogel-like (Low Density and High Surface Area) Cellulose Monoliths and Beads Obtained without Supercritical- or Freeze-Drying. *Cellulose* **2023**, 30, 8339–8353. DOI: 10.1007/s10570-023-05349-8.
(36) Lide, D. R. *CRC Handbook of Chemistry and Physics, 85th Edition*; CRC Press, 2004.
(37) Druel, L. Cellulose based aerogels: properties and shaping as beads. Ph.D. Dissertation, Mines ParisTech/Université Paris Sciences et Lettres, 2019. https://pastel.hal.science/tel-02434794
(38) Groult, S.; Budtova, T. Tuning Structure and Properties of Pectin Aerogels. *Eur. Polym. J.* **2018**, *108*, 250–261. DOI: 10.1016/j.eurpolymj.2018.08.048.
(39) Rudaz, C.; Courson, R.; Bonnet, L.; Calas-Etienne, S.; Sallée, H.; Budtova, T. Aeropectin: Fully Biomass-Based Mechanically Strong and Thermal Superinsulating Aerogel. *Biomacromolecules* **2014**, *15* (6), 2188–2195. DOI: 10.1021/bm500345u.

(40) Mao, Y.; Zhou, J.; Cai, J.; Zhang, L. Effects of Coagulants on Porous Structure of Membranes Prepared from Cellulose in NaOH/Urea Aqueous Solution. *J. Membr. Sci.* **2006**, *279* (1), 246–255. DOI: 10.1016/j.memsci.2005.07.048.
(41) Karna, N. K.; Kozlowski, A. M.; Hasani, M. Unraveling the Thermodynamics of the CO2 Driven Precipitation of Cellulose in Aqueous NaOH. *Chem. Phys.* **2023**, *575*, 112060. DOI: 10.1016/j.chemphys.2023.112060.
(42) Gavillon, R.; Budtova, T. Kinetics of Cellulose Regeneration from Cellulose−NaOH−Water Gels and Comparison with Cellulose−N-Methylmorpholine-N-Oxide−Water Solutions. *Biomacromolecules* **2007**, *8* (2), 424–432. DOI: 10.1021/bm060376q.
(43) Li, H.; Kruteva, M.; Mystek, K.; Dulle, M.; Ji, W.; Pettersson, T.; Wågberg, L. Macro- and Microstructural Evolution during Drying of Regenerated Cellulose Beads. *ACS Nano* **2020**, *14* (6), 6774–6784. DOI: 10.1021/acsnano.0c00171.
(44) Zou, F.; Budtova, T. Starch Alcogels, Aerogels, and Aerogel-like Xerogels: Adsorption and Release of Theophylline. *ACS Sustainable Chem. Eng.* **2023**, *11* (14), 5617–5625. DOI: 10.1021/acssuschemeng.2c07762.
(45) Isobe, N.; Kim, U.-J.; Kimura, S.; Wada, M.; Kuga, S. Internal Surface Polarity of Regenerated Cellulose Gel Depends on the Species Used as Coagulant. *J. Colloid Interface Sci.* **2011**, *359* (1), 194–201. DOI: 10.1016/j.jcis.2011.03.038.
(46) Nunes, C.; Mahendrasingam, A.; Suryanarayanan, R. Investigation of the Multi-Step Dehydration Reaction of Theophylline Monohydrate Using 2-Dimensional Powder X-Ray Diffractometry. *Pharm Res* **2006**, *23* (10), 2393–2404. DOI: 10.1007/s11095-006-9022-5.
(47) Zhu, M.; Wang, Y.; Li, F.; Bao, Y.; Huang, X.; Shi, H.; Hao, H. Theoretical Model and Experimental Investigations on Solution-Mediated Polymorphic Transformation of Theophylline: From Polymorph I to Polymorph II. *Crystals* **2019**, *9* (5), 260. DOI: 10.3390/cryst9050260.
(48) Chartier, C.; Buwalda, S.; Ilochonwu, B. C.; Van Den Berghe, H.; Bethry, A.; Vermonden, T.; Viola, M.; Nottelet, B.; Budtova, T. Release Kinetics of Dexamethasone Phosphate from Porous Chitosan: Comparison of Aerogels and Cryogels. *Biomacromolecules* **2023**. 24 (10), 4494-4501. DOI: 10.1021/acs.biomac.2c01408.
(49) Washburn, E. W. The Dynamics of Capillary Flow. *Phys. Rev.* **1921**, *17* (3), 273–283. DOI: 10.1103/PhysRev.17.273.
(50) Luukkonen, P.; Maloney, T.; Rantanen, J.; Paulapuro, H.; Yliruusi, J. Microcrystalline Cellulose-Water Interaction—A Novel Approach Using Thermoporosimetry. *Pharm Res* **2001**, *18* (11), 1562–1569. DOI: 10.1023/A:1013030414555.
(51) Jeffries, R. The Amorphous Fraction of Cellulose and Its Relation to Moisture Sorption. *J. Appl. Polym. Sci.* **1964**, *8* (3), 1213–1220. DOI: 10.1002/app.1964.070080314.
(52) Kocherbitov, V.; Ulvenlund, S.; Kober, M.; Jarring, K.; Arnebrant, T. Hydration of Microcrystalline Cellulose and Milled Cellulose Studied by Sorption Calorimetry. *J. Phys. Chem. B* **2008**, *112* (12), 3728–3734. DOI: 10.1021/jp711554c.
(53) Huang, X.; Brazel, C. S. On the Importance and Mechanisms of Burst Release in Matrix-Controlled Drug Delivery Systems. *J. Controlled Release* **2001**, *73* (2), 121–136. DOI: 10.1016/S0168-3659(01)00248-6.
(54) Higuchi, T. Mechanism of Sustained-Action Medication. Theoretical Analysis of Rate of Release of Solid Drugs Dispersed in Solid Matrices. *J. Pharm. Sci.* **1963**, *52* (12), 1145–1149. DOI: 10.1002/jps.2600521210.

(55) Frenning, G. Modelling Drug Release from Inert Matrix Systems: From Moving-Boundary to Continuous-Field Descriptions. *Int. J. Pharm*. **2011**, *418* (1), 88–99. DOI: 10.1016/j.ijpharm.2010.11.030.

Supporting Information

From cellulose solutions to aerogels and xerogels: controlling properties for drug delivery

Loris Gelas, Tatiana Budtova*

Mines Paris, PSL University, Center for Materials Forming (CEMEF), UMR CNRS 7635, CS 10207, 06904 Sophia Antipolis, France

Corresponding author: Tatiana Budtova

Tatiana.budtova@minesparis.psl.eu

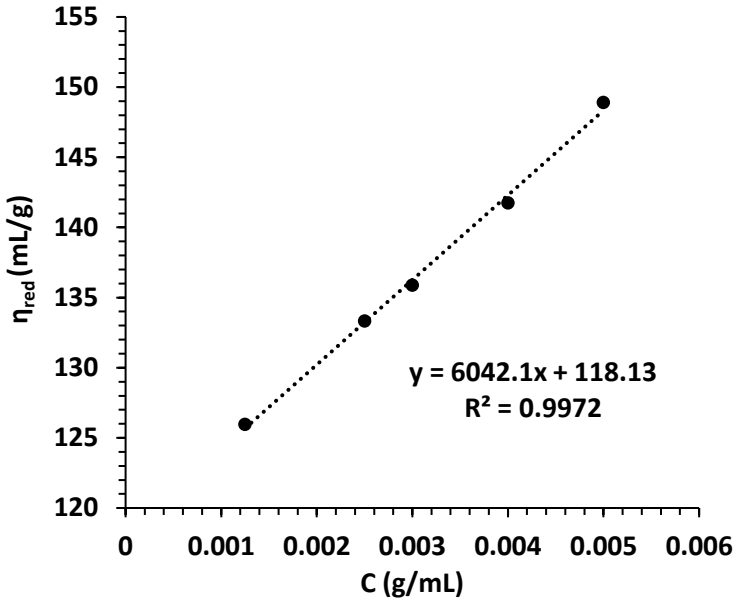

Figure S8

Determination of intrinsic viscosity of microcrystalline cellulose in 0.5 M cupryethylenediamine (η_{red} is reduced viscosity and C cellulose concentration)

The viscosity average degree of polymerization ($\overline{\overline{P_v}}$) was determined using Mark-Houwink-Sakurada equation:

$$[\eta] = K\overline{P_v^a}$$

where [η] is intrinsic viscosity, K and *a* are empirical constants equal to 0.806 and 1.26, respectively[1]. Intrinsic viscosity was found to be 118.13 g/mL and $\overline{\overline{P_v}}$ 280.

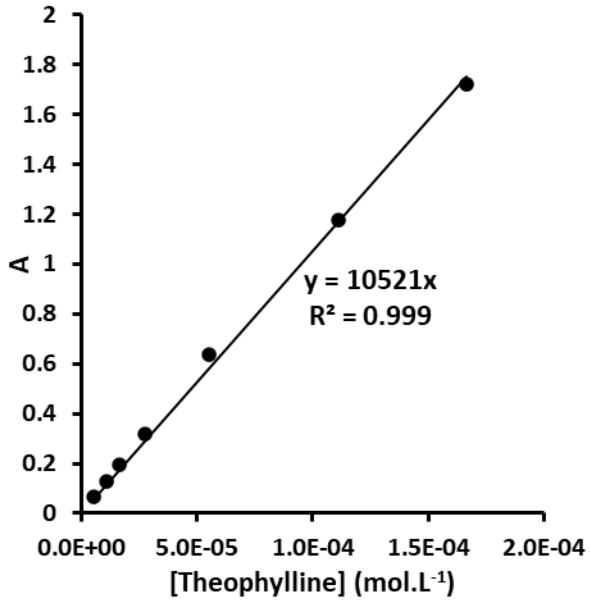

Figure S2

Calibration dependence for the determination of molar extinction coefficient of theophylline by spectrophotometry

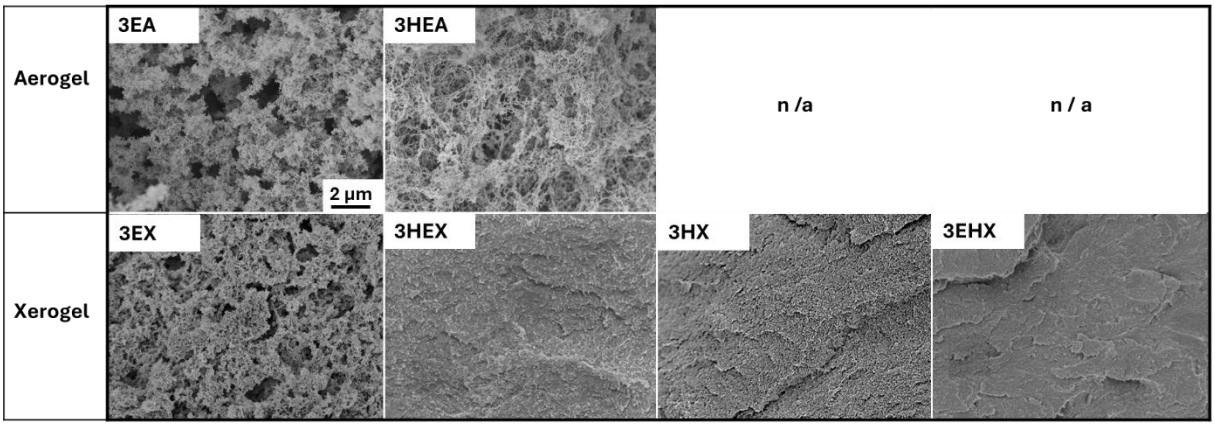

Figure S3

Morphology of cellulose materials made from 3%cellulose/8%NaOH/water solutions; the scale is the same for all images

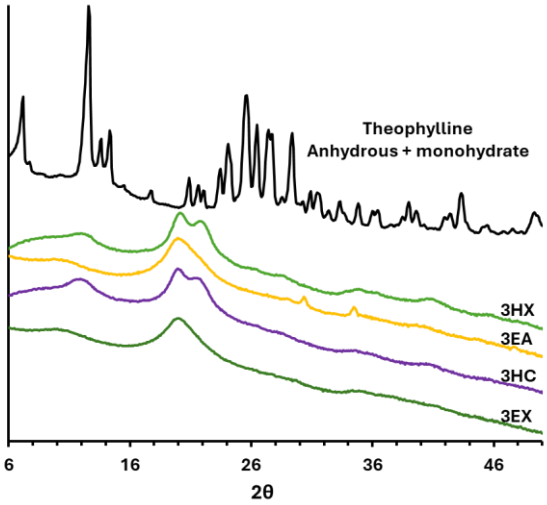

Figure S4.

XRD pattern of theophylline (2 allomorphs are present: theophylline monohydrate and anhydrous theophylline) and of dry cellulose samples containing theophylline.

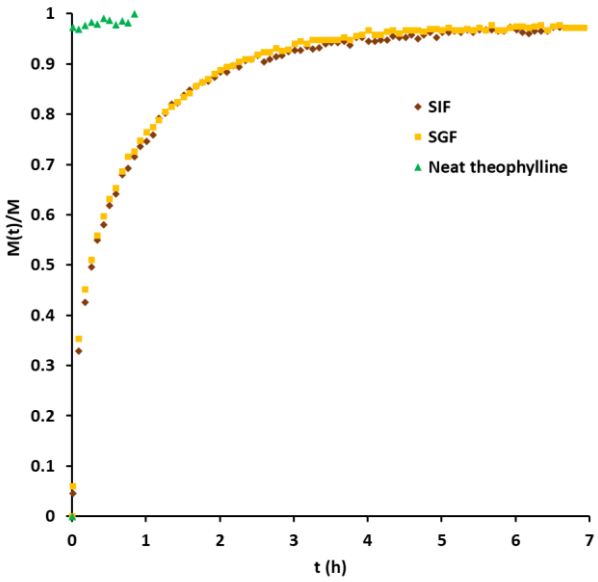

Figure S5.

Dissolution kinetics of neat theophylline (green triangles) and release kinetics of theophylline from 3HA into simulated intestinal fluid (SIF) alone and into simulated gastric fluid (SGF) alone

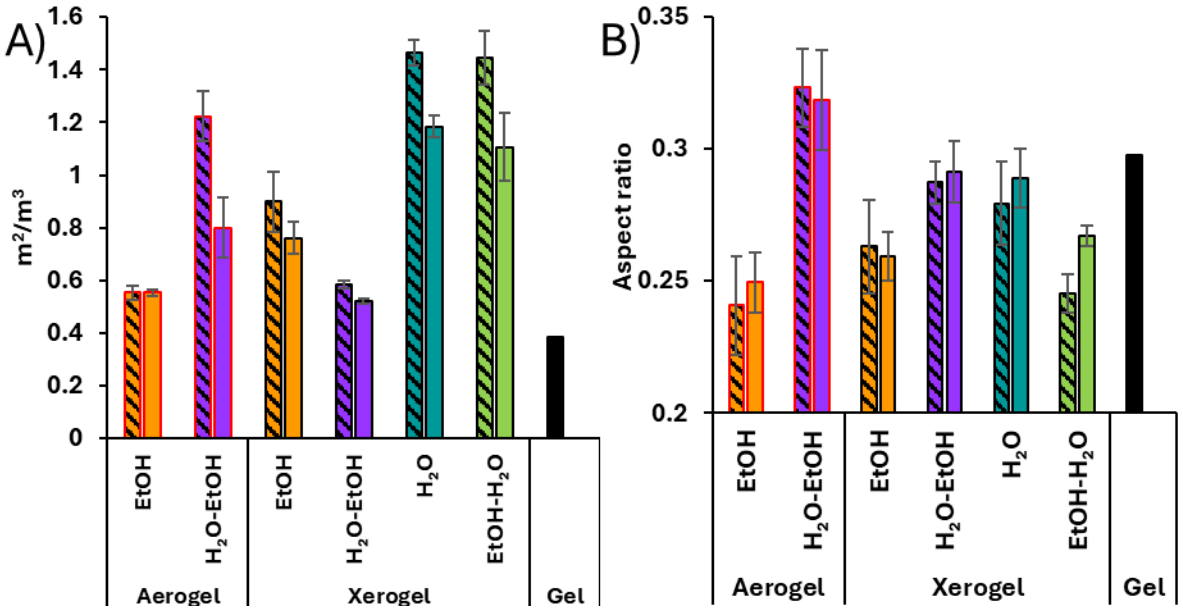

Figure S6

Sample external surface to volume ratio (A) and aspect ratio (B)

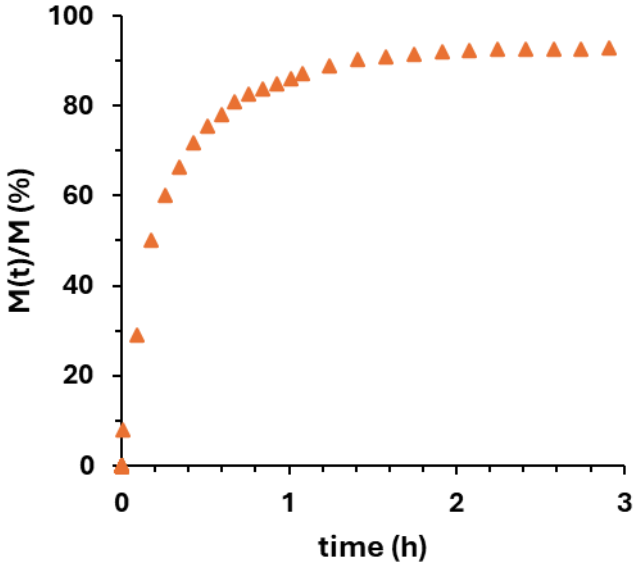

Figure S7

Example of theophylline release kinetics from 3EA aerogel.

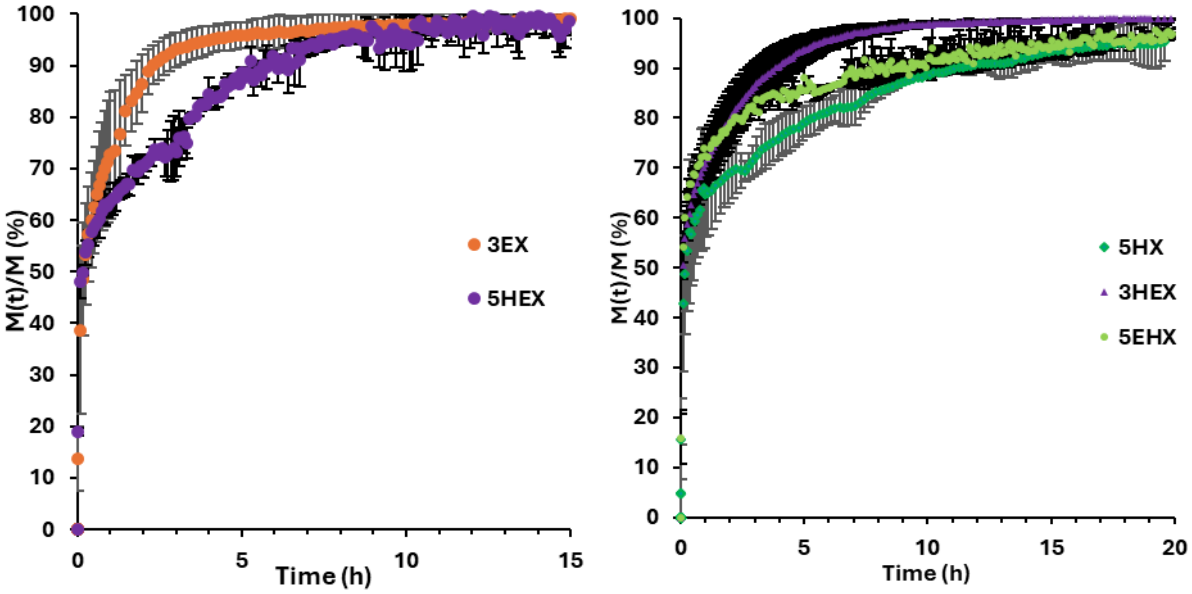

Figure S8

Reproduction of Figure 7 with error bars.

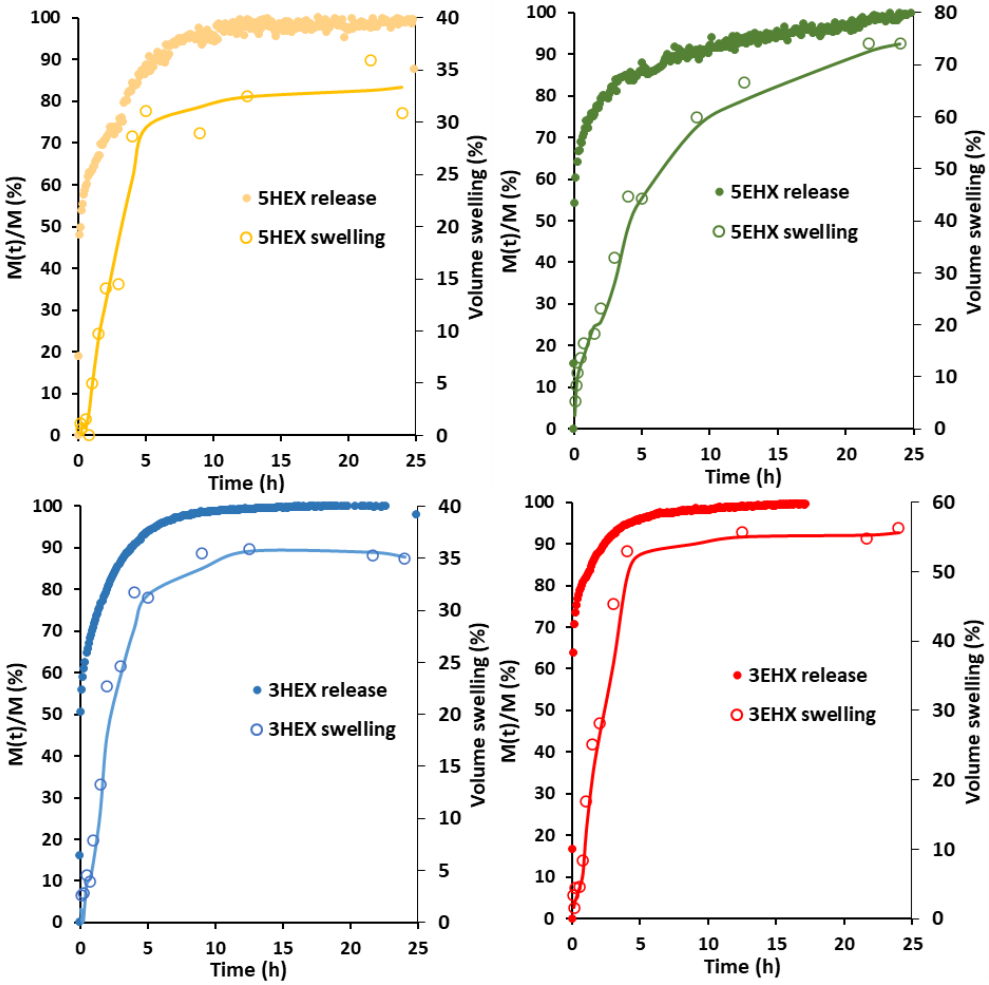

Figure S9

Correlation between kinetics of theophylline release and cellulose sample swelling for low-porosity xerogels. Obtained by letting the dry material in sink conditions in SGF for one hour and in SIF for 24 h, regularly measuring volume using caliper, the results shown here are average from two different measurements.

Reference:

1. Evans, R. & Wallis, A. F. A. Cellulose molecular weights determined by viscometry. *Journal of Applied Polymer Science* **37**, 2331–2340 (1989).